Electron-impact excitation of O III in the distorted-wave approximation

Michael S. Pindzola

Theoretical Studies Group, Goddard Space Flight Center, National Aeronautics and Space Administration,
Greenbelt, Maryland 20771
(Received 14 January 1977)

The $^3P \rightarrow {}^1D$ electron-impact excitation cross section within the ground configuration of doubly ionized oxygen is calculated in the distorted-wave approximation. An essential element of the present treatment is that we do not assume orthogonality between core and scattering orbitals of the same angular symmetry. Resonance structures are included through the use of quantum defect theory. Near threshold the effect of an isolated autoionization resonance in the dominant $^2D^o$ partial wave is found to be important, in agreement with previous close-coupling results.

I. INTRODUCTION

Theoretical calculation of atomic collision processes is important in understanding the behavior of astrophysical and laboratory plasmas. For electron-impact excitation of positive ions, theoretical knowledge is crucial since accurate experiments are difficult for multiply charged ions.[1] Near threshold for excitation, which is usually the energy region of prime interest, the incident electron and the atomic electrons have velocities that are comparable. For this energy range, strong-coupling methods[2] employing a partial-wave expansion of the scattered electron should be used.

In electron scattering from neutral atoms, resonances can occur just below the energies of excited states of the target atom. For electron excitation of positive ions the energies of these autoionization resonances can descend very far below the parent excited state, in fact even far below lower excited states of the target ion. For highly charged ions, a full close-coupling calculation becomes impractical since one is forced to include many resonant closed channels even near the threshold for excitation. The distorted-wave method, with its numerical simplicity and fast computational speed, becomes a reasonable alternative.

In recent years the distorted-wave method has been applied to the calculation of resonant structures in electron-impact excitation of ions. Using distorted waves calculated in a suitable central potential, Hershkowitz and Seaton[3] found resonance effects in the excitation cross sections for carbon III and oxygen V to be quite important. Using essentially only Coulomb waves, Presnyakov and Urnov[4] have also found average resonance effects to be very large in various excitations of oxygen VI.

In this paper we try to ascertain the accuracy of the distorted-wave method by calculating the low-energy resonance structures in the $^3P \rightarrow {}^1D$ transition within the ground configuration of oxygen III. The distorted-wave equations are derived using the Kohn variational principle in which we do not assume orthogonality between core and scattering orbitals of the same angular symmetry.[5] Thus the distorted waves incorporate exchange effects in a fully consistent way. In Sec. II we review the resonant structure theory. Our distorted-wave results for oxygen III are then given in Sec. III along with a comparison to an elaborate configuration-interaction close-coupling calculation.[6] Section IV contains a brief summary.

II. RESONANCE STRUCTURE THEORY

The general theory of the distorted-wave method as applied to atomic collisions is well known. In this paper we use the distorted-wave approximation to the close-coupling expansion for the total wave function Ψ as presented by Mott and Massey.[7] This formulation seems especially appropriate when the energy separation between initial and final states of the atom is small compared to the ionization potential.

The expansion of the total wave function Ψ is in a representation $(nL_n S_n k_n l_n s L S M_l M_s \Pi)$ in which the orbital and spin angular momenta of the scattered electron $(k_n l_n s)$ and the atom $(n L_n S_n)$ are coupled together. One assumes that the total and component orbital- and spin-angular-momentum quantum numbers L, S, M_l, M_s, as well as parity Π, are conserved during the collision. The generalized Hartree-Fock coupled equations for Ψ are derived from the Kohn variational principle, where no orthogonality restrictions are made on core and scattering orbitals of the same angular symmetry. For a fixed set of conserved quantum numbers $\Gamma = LS\Pi$, the set of radial-coupled integro-differential equations have the general form

$$[T_{l_i} - 2V_{ii}^\Gamma(r) + k_i^2]F_{ii'}^\Gamma(r) = \sum_{\substack{j=1 \\ j \neq i}}^{N} 2V_{ij}^\Gamma(r)F_{ji'}^\Gamma(r) \Bigg|_{i=1,N} ,$$

$$(1)$$

where

$$T_{l_i} = \frac{d^2}{dr^2} - \frac{l_i(l_i+1)}{r^2} + \frac{2Z}{r} , \qquad (2)$$

$\frac{1}{2}k_i^2$ is the energy, Z is the atomic number, and atomic units (1 a.u. = 27.21 eV) are used. The index i in Eq. (1) runs over all N channels in the expansion, while i' specifies the initial conditions. The potentials $V_{ij}^\Gamma(r)$ contain both direct and exchange integrals.

By dropping all terms involving coupling potentials in Eq. (1) we obtain the distorted-wave equations

$$[T_{l_i} - 2V_{ii}^\Gamma(r) + k_i^2]f_i^\Gamma(r) = 0 \big|_{i=1,N} . \qquad (3)$$

The scattering orbitals $f_i^\Gamma(r)$ are given the normalization

$$f_i^\Gamma(r) \xrightarrow[r \to \infty]{} \sin(k_i x + \delta_i) , \qquad (4)$$

where

$$k_i x = k_i r - \tfrac{1}{2}l_i \pi + (z/k_i)\ln(2k_i r) + \sigma_i , \qquad (5)$$

z is the residual charge on the atom, σ_i is the Coulomb phase shift, and δ_i is the non-Coulomb phase shift.

The asymptotic form of the radial functions $F_{ii'}^\Gamma(r)$ of Eq. (1), for all N channels open, may be written as

$$F_{ii'}^\Gamma(r) \underset{r \to \infty}{\sim} (1/\sqrt{k_i})\{\delta_{ii'}e^{-i(k_i x + \delta_i)} - S_{ii'}^\Gamma e^{i(k_i x + \delta_i)}\} . \qquad (6)$$

The S^Γ matrix in the distorted-wave approximation takes the form

$$S^\Gamma \cong \begin{bmatrix} 1+\Delta(1) & S_{12}^\Gamma & \cdots & S_{1N}^\Gamma \\ S_{21}^\Gamma & 1+\Delta(2) & & \cdot \\ \cdot & & & \cdot \\ \cdot & & & \cdot \\ \cdot & & & \cdot \\ S_{N1}^\Gamma & \cdots & & 1+\Delta(N) \end{bmatrix} , \qquad (7)$$

where

$$\Delta(i) = \frac{1}{2}\sum_{\substack{j=1 \\ j \neq i}}^{N} [S_{ij}^\Gamma]^2 , \qquad (8)$$

and (see Chap. 4 of Mott and Massey[7])

$$S_{ij}^\Gamma \big|_{i \neq j} = \frac{4}{i(k_i k_j)^{1/2}} \int_0^\infty f_i^\Gamma(r) V_{ij}^\Gamma(r) f_j^\Gamma(r) \, dr . \qquad (9)$$

The form of the diagonal elements in Eq. (7) is equivalent to that given by Seaton.[8] In particular, the $\Delta(i)$ contribution is necessary in order to retain information about the resonance widths.

When some channels are closed, we may use the results of quantum-defect theory to calculate the S^Γ matrix with M open channels $(M < N)$.[1] We use Latin letters for open channels $(1 \leq i,j,\ldots \leq M)$ and Greek letters for closed channels $(M+1 \leq \alpha,\beta,\ldots \leq N)$. For closed channels $\alpha = M+1$ to N, the distorted-wave equations (3) are solved at negative energies given by

$$k_\alpha^2/2 = -z^2/2\nu_\alpha^2 , \qquad (10)$$

where ν_α is the effective quantum number. The eigenfunctions $P_{\alpha,n}^\Gamma(r)$ of the distorted-wave equations are bound scattering orbitals attached to excited states of the atom and thus may produce autoionization resonances in the excitation cross sections. The eigenenergies are given by $-z^2/2\nu_{\alpha,n}^2$ and the quantum defect $\mu_{\alpha,n}$ is defined by

$$\mu_{\alpha,n} = n - \nu_{\alpha,n} , \qquad (11)$$

where $\mu_{\alpha,n}$ is of course a slowly varying function of n. As has been shown,[3] the analytically continued function $f_{\alpha,n}^\Gamma(r)$, at the eigenenergy $-z^2/2\nu_{\alpha,n}^2$, is related to the orthonormalized eigenfunction $P_{\alpha,n}^\Gamma(r)$ by

$$f_{\alpha,n}^\Gamma(r) = (i\pi\nu_{\alpha,n}^2/2z)^{1/2}\theta_\alpha P_{\alpha,n}^\Gamma(r) , \qquad (12)$$

where θ_α is generally close to unity.[3]

We now analytically continue S^Γ of Eq. (7) into an N-dimensional matrix $\mathcal{S}^\Gamma$. Using Eqs. (8), (9), and (12) the elements of the $\mathcal{S}^\Gamma$ matrix are given by

$$\mathcal{S}_{ij}^\Gamma \big|_{i \neq j} = \frac{4}{i(k_i k_j)^{1/2}} \int_0^\infty f_i^\Gamma(r) V_{ij}^\Gamma(r) f_j^\Gamma(r) \, dr , \qquad (13)$$

$$\mathcal{S}_{i\alpha}^\Gamma = \frac{4}{i\sqrt{k_i}} \left(\frac{\pi\nu_\alpha^3}{2z^2}\right)^{1/2} \int_0^\infty f_i^\Gamma(r) V_{i\alpha}^\Gamma(r) P_{\alpha,n}^\Gamma(r) \, dr , \qquad (14)$$

$$\mathcal{S}_{\alpha\beta}^\Gamma \big|_{\alpha \neq \beta} = \frac{2\pi}{iz^2} (\nu_\alpha \nu_\beta)^{3/2} \int_0^\infty P_{\alpha,n}^\Gamma(r) V_{\alpha\beta}^\Gamma(r) P_{\beta,n'}^\Gamma(r) \, dr , \qquad (15)$$

$$\mathcal{S}_{ii}^\Gamma = 1 + \tilde{\Delta}(i) , \qquad (16)$$

$$\mathcal{S}_{\alpha\alpha}^\Gamma = 1 + \tilde{\Delta}(\alpha) , \qquad (17)$$

where

$$\tilde{\Delta}(i) = \frac{1}{2}\left(\sum_{\substack{j=1 \\ j \neq i}}^{M} [\mathcal{S}_{ij}^\Gamma]^2 + \sum_{\alpha=M+1}^{N} [\mathcal{S}_{i\alpha}^\Gamma]^2\right) \qquad (18)$$

and

$$\tilde{\Delta}(\alpha) = \frac{1}{2}\left(\sum_{j=1}^{M} [\mathcal{S}_{\alpha j}^\Gamma]^2 + \sum_{\substack{\beta=M+1 \\ \beta \neq \alpha}}^{N} [\mathcal{S}_{\alpha\beta}^\Gamma]^2\right) . \qquad (19)$$

The specific eigenfunction $P_{\alpha,n}^\Gamma(r)$ is taken as the one whose eigenenergy $-z^2/2\nu_{\alpha,n}^2$ lies closest in energy to $-z^2/2\nu_\alpha^2$. Alternatively,[4] one can calcu-

late a function $f_\alpha^\Gamma(r)$ [or $P_\alpha^\Gamma(r)$] for all energies. The function $f_\alpha^\Gamma(r)$ at noneigenenergies increases exponentially at large distances. An appropriate convergence factor $(\lim_{b\to 0} e^{-br^2})$ must then be used to define a norm for the state.[9]

The fundamental equation of quantum-defect

$$
\mathfrak{X}^\Gamma =
\begin{bmatrix}
S_{M+1,M+1}^\Gamma - \Omega(M+1) & S_{M+1,M+2}^\Gamma & \cdots & S_{M+1,N}^\Gamma \\
S_{M+2,M+1}^\Gamma & S_{M+2,M+2}^\Gamma - \Omega(M+2) & & \vdots \\
\vdots & & & \vdots \\
S_{N,M+1}^\Gamma & \cdots & & S_{N,N}^\Gamma - \Omega(N)
\end{bmatrix}
, \tag{21}
$$

$$
\Omega(\alpha) = \exp[-2i(\pi\nu_\alpha + \delta_\alpha)], \tag{22}
$$

and the analytic continuation of the phase shift δ_α is $\pi\mu_\alpha$.

The total excitation cross section σ (in units of πa_0^2) for the transition $nL_iS_i \to n'L_jS_j$ is given by[10]

$$
\sigma = \sum_{LS l_i l_j} \sigma(\Gamma, l_i \to l_j), \tag{23}
$$

where

$$
\sigma(\Gamma, l_i \to l_j) = \frac{(2L+1)(2S+1)}{2k_i^2(2L_i+1)(2S_i+1)} |S_{ji}^\Gamma|^2. \tag{24}
$$

If we limit our consideration to a three-channel problem in which the excitation $1 \to 2$ proceeds in the presence of a single closed channel 3, we may write Eq. (20) as

$$
S_{21}^\Gamma = S_{21}^\Gamma - S_{23}^\Gamma S_{31}^\Gamma / [S_{33}^\Gamma - \Omega(3)]. \tag{25}
$$

Since

$$
\nu_3 + \mu_3 = \nu_{3,n} + (\nu_3 - \nu_{3,n}) + \mu_3 = n + (\nu_3 - \nu_{3,n}),
$$

where $\nu_{3,n}$ is the eigen-quantum-number closest to ν_3, we may write[8]

$$
S_{33}^\Gamma - \Omega(3) \cong [1 + \tilde{\Delta}(3)] - [1 - 2i\pi(\nu_3 - \nu_{3,n})]
$$

$$
= 2i\pi[\nu_3 - \nu_{3,n} - (i/2\pi)\tilde{\Delta}(3)]. \tag{26}
$$

Equation (25) now takes the form

$$
S_{21}^\Gamma = 2i\left(A - \frac{B}{\nu_3 - \nu_{3,n} + iG}\right), \tag{27}
$$

where

$$
A = \frac{S_{21}^\Gamma}{2i}, \quad B = -\frac{S_{23}^\Gamma S_{31}^\Gamma}{4\pi}, \quad G = -\frac{1}{4\pi}\sum_{i=1}^{2}[S_{3i}^\Gamma]^2.
$$

One should note that A, B, and G are all real quantities. Substituting Eq. (27) into Eq. (24), we

theory is that the elements of the S^Γ matrix with M open channels are given by[1]

$$
S_{ij}^\Gamma = S_{ij}^\Gamma - \sum_{\alpha=M+1}^{N} \sum_{\beta=M+1}^{N} S_{i\alpha}^\Gamma [\mathfrak{X}_{\alpha\beta}^\Gamma]^{-1} S_{\beta j}^\Gamma, \tag{20}
$$

where

obtain for the partial-wave excitation $(1 \to 2)$ cross section in the presence of a closed channel 3:

$$
\sigma(\Gamma, l_1 \to l_2) = \frac{2(2L+1)(2S+1)}{k_1^2(2L_1+1)(2S_1+1)}
$$

$$
\times \left[A^2 + \frac{B^2 - 2AB(\nu_3 - \nu_{3,n})}{(\nu_3 - \nu_{3,n})^2 + G^2}\right]. \tag{28}
$$

If only the first term inside the brackets of Eq. (28) is kept, we retain the nonresonant excitation cross section. The second term inside the brackets gives rise to an infinite series of resonances converging to the threshold of excitation of channel 3. The Gailitis resonance-averaged cross section, $\langle\sigma(\Gamma, l_1 \to l_2)\rangle$,[11] is found from

$$
\langle\sigma(\Gamma, l_1 \to l_2)\rangle = \int_{\nu_{3,n}-1/2}^{\nu_{3,n}+1/2} \sigma(\Gamma, l_1 \to l_2)\, d\nu_3. \tag{29}
$$

Substituting Eq. (28) into (29) and performing the integration, we obtain

$$
\langle\sigma(\Gamma, l_1 \to l_2)\rangle = \frac{2(2L+1)(2S+1)}{k_1^2(2L_1+1)(2S_1+1)} \left[A^2 + \frac{\pi B^2}{G}\right]. \tag{30}
$$

We may extend our consideration to a problem in which the excitation $1 \to 2$ proceeds in the presence of many closed channels α. Neglecting the off-diagonal elements of the $\mathfrak{X}^\Gamma$ matrix of Eq. (21), we may write Eq. (20) as

$$
S_{21}^\Gamma = S_{21}^\Gamma - \sum_{\alpha=3}^{N} \frac{S_{2\alpha}^\Gamma S_{\alpha 1}^\Gamma}{2i\pi[\nu_\alpha - \nu_{\alpha,n} - (i/2\pi)\tilde{\Delta}(\alpha)]}. \tag{31}
$$

This is a quite accurate approximation for non-overlapping resonances associated with different ion levels. Although for a group of degenerate closed channels (i.e., more than one value of l_α is

allowed for fixed values of S_α, L_α, S, L, and Π) one should change to a representation in which the matrix

$$\mathcal{Y}^\Gamma = \begin{bmatrix} \mathcal{S}^\Gamma_{3,3} & \cdots & \mathcal{S}^\Gamma_{3,N} \\ \cdot & & \\ \cdot & & \\ \cdot & & \\ \mathcal{S}^\Gamma_{N,3} & \cdots & \mathcal{S}^\Gamma_{N,N} \end{bmatrix} \qquad (32)$$

is diagonal (thus obtaining complex quantum defects)[8], Eq. (31) is still a fairly good approximation. Expressions for $\sigma(\Gamma, l_1 \to l_2)$ and $\langle \sigma(\Gamma, l_1 \to l_2) \rangle$ may be easily derived from Eq. (31).

III. CALCULATION FOR OXYGEN iii

In this section we apply the distorted-wave resonance structure theory of Sec. II to the calculation of the $^3P \to {}^1D$ electron excitation cross section within the ground configuration of doubly ionized oxygen. The single-particle core orbitals for the ground ^3P state of oxygen III were calculated numerically[12] in the Hartree-Fock approximation using only the single configuration $1s^2 2s^2 2p^2$. As previously found,[5,6] it is a good approximation to use these same radial orbitals for all low-lying excited atomic states of oxygen III. The scattering orbitals were computed for different partial waves

using Eq. (3) with

$$V^\Gamma(r) = \sum_{nl}\sum_\kappa (C^D_{nl}J^\kappa_{nl} + C^E_{nl}K^\kappa_{nl}) + C^{EO}_{n_0 l_0}I_{n_0 l_0}, \qquad (33)$$

where explicit coefficients C_{nl} for the various direct J^κ_{nl} and exchange K^κ_{nl} potentials are given in Table I. The exchange-overlap $I_{n_0 l_0}$ potential is a consequence of the nonorthogonality of core and scattering orbitals of the same angular symmetry.[5] Experimental removal energies[13] are used in all cases in order to have the excitation thresholds agree with experiment. States labeled kl are calculated at positive energies $k^2/2$, while those labeled vl are calculated at negative energies $\epsilon_v = -z^2/2v^2$. The $\mathcal{S}^\Gamma$ matrix elements were computed for different partial-wave transitions using Eqs. (13) and (14), where the radial integrals over the various coupling potentials for $^2D^o$ and $^2P^o$ are explicitly given in Table II.

Owing to the spin-forbidden nature of the $^3P \to {}^1D$ transition, convergence of the partial-wave expansion is rapid. In the low-energy region from the ^1D threshold (at 2.51 eV[13]) to 5.0 eV, the largest partial-wave cross section $\sigma(^2D^o, p \to p)$ is dominated by the resonance effects of an O II $1s^2 2s 2p^3$ ^3D $3s$ $^2D^o$ autoionization state. Using Eq. (3) and Table I we calculated the $3s$ orbital using a fixed core and found the energy to be $\epsilon_v = 4.20$ eV relative to the ^3P ground state. The threshold for the opening of the $1s^2 2s 2p^3$ ^3D channel is at 14.88 eV.[13] This is an excellent illustration of how far autoionization states can descend below the parent

TABLE I. Scattering orbital configurations, terms, and potentials.

State	cJ^κ_{1s}[a] c	κ	cK^κ_{1s}[b] c	κ	cJ^κ_{2s} c	κ	cK^κ_{2s} c	κ	cI_{2s}[c] c	cJ^κ_{2p} c	κ	cJ^κ_{2p} c	κ	cK^κ_{2p} c	κ	cK^κ_{2p} c	κ	cI_{2p} c
$2s^2 2p^2\,{}^3P\,kp\,{}^2D^o$	2	0	$-\frac{1}{3}$	1	2	0	$-\frac{1}{3}$	1		2	0	$-\frac{1}{25}$	2	$\frac{1}{2}$	0	$\frac{2}{25}$	2	$\frac{1}{2}(\epsilon^{3P}_{2p}-\epsilon_k)$
$2s^2 2p^2\,{}^1D\,kp\,{}^2D^o$	2	0	$-\frac{1}{3}$	1	2	0	$-\frac{1}{3}$	1		2	0	$-\frac{7}{25}$	2	$\frac{1}{2}$	0	$-\frac{4}{25}$	2	$\frac{1}{2}(\epsilon^{1D}_{2p}-\epsilon_k)$
$2s 2p^3\,{}^3D\,vs\,{}^2D^o$	2	0	-1	0	1	0	$+\frac{1}{2}$	0	$\frac{1}{2}(\epsilon^{3D}_{2s}-\epsilon_v)$	3	0			$-\frac{1}{6}$	1			
$2s^2 2p^2\,{}^3P\,kp\,{}^2P^o$	2	0	$-\frac{1}{3}$	1	2	0	$-\frac{1}{3}$	1		2	0	$\frac{1}{5}$	2	$\frac{1}{2}$	0	$\frac{1}{5}$	2	$\frac{1}{2}(\epsilon^{3P}_{2p}-\epsilon_k)$
$2s^2 2p^2\,{}^1D\,kp\,{}^2P^o$	2	0	$-\frac{1}{3}$	1	2	0	$-\frac{1}{3}$	1		2	0	$\frac{7}{25}$	2	$-\frac{1}{6}$	0	$-\frac{23}{75}$	2	$-\frac{1}{6}(\epsilon^{3P}_{2p}-\epsilon_k)$
$2s^2 2p^2\,{}^1S\,vp\,{}^2P^o$	2	0	$-\frac{1}{3}$	1	2	0	$-\frac{1}{3}$	1		2	0			$-\frac{1}{3}$	0	$-\frac{2}{15}$	2	$-\frac{1}{3}(\epsilon^{1S}_{2p}-\epsilon_v)$
$2s^2 2p^2\,{}^3P\,kd\,{}^2F^e$	2	0	$-\frac{1}{5}$	2	2	0	$-\frac{1}{5}$	2		2	0	$-\frac{2}{35}$	2	$\frac{1}{5}$	1	$\frac{9}{245}$	3	
$2s^2 2p^2\,{}^1D\,kd\,{}^2F^e$	2	0	$-\frac{1}{5}$	2	2	0	$-\frac{1}{5}$	2		2	0	$-\frac{8}{35}$	2			$\frac{3}{49}$	3	
$2s^2 2p^2\,{}^3P\,kd\,{}^2P^e$	2	0	$-\frac{1}{5}$	2	2	0	$-\frac{1}{5}$	2		2	0	$-\frac{1}{5}$	2	$-\frac{2}{15}$	1	$\frac{9}{70}$	3	
$2s^2 2p^2\,{}^1D\,kd\,{}^2P^e$	2	0	$-\frac{1}{5}$	2	2	0	$-\frac{1}{5}$	2		2	0	$\frac{1}{5}$	2			$-\frac{3}{14}$	3	

[a]Direct potential $J^\kappa_{nl}f_{kl}(r) = \int_0^\infty P^2_{nl}(r')(r^\kappa_</r^{\kappa+1}_>)dr'\, f_{kl}(r)$.

[b]Exchange potential $K^\kappa_{nl}f_{kl}(r) = \int_0^\infty P_{nl}(r')f_{kl}(r')(r^\kappa_</r^{\kappa+1}_>)dr'\, P_{nl}(r)$.

[c]Exchange-overlap potential $I_{nl}f_{kl}(r) = \int_0^\infty P_{nl}(r')f_{kl}(r')dr'\, P_{nl}(r)$.

TABLE II. Radial integrals of coupling potentials.

Partial wave	Transition	Form of matrix elements
$^2D^o$	$^3P k_1 p \to {}^1D k_2 p$	$-\frac{3}{2}\langle 2p k_2 p | v0 | k_1 p 2p \rangle^a + \frac{3}{25}\langle 2p k_2 p | v2 | k_1 p 2p \rangle^b - \frac{3}{2}(\epsilon_{2p}^{1D} - \frac{1}{2}k_1^2)\langle k_2 p | 2p \rangle \langle 2p | k_1 p \rangle$
	$^3D_3 s \to {}^1D k_2 p$	$-\frac{3}{2}\langle 2s k_2 p | v0 | \nu_3 s 2p \rangle - \frac{3}{2}(\epsilon_{2s}^{1D} + z^2/2\nu_3^2)\langle 2s p | 2p \rangle \langle 2s | \nu_3 s \rangle + \Lambda_1^c$
	$^1P k_1 p \to {}^3D \nu_3 s$	$-\frac{1}{3}\langle \nu_3 s 2p | v1 | k_1 p 2s \rangle + \frac{3}{2}\langle 2p \nu_3 s | v0 | k_1 p 2s \rangle + \frac{3}{2}(\epsilon_{2s}^{3P} + z^2/2\nu_3^2)\langle \nu_3 s | 2s \rangle \langle 2p | k_1 p \rangle + \Lambda_2$
$^2P^o$	$^3P k_1 p \to {}^1D k_2 p$	$(5/4)^{1/2}\langle 2p k_2 p | v0 | k_1 p 2p \rangle + (4/125)^{1/2}\langle 2p k_2 p | v2 | k_1 p 2p \rangle + (5/4)^{1/2}(\epsilon_{2p}^{1D} - k_1^2/2)\langle k_2 p | 2p \rangle \langle 2p | k_1 p \rangle$
	$^1S \nu_3 p \to {}^1D k_2 p$	$(16/125)^{1/2}\langle k_2 p 2p | v2 | \nu_3 p 2p \rangle - (5/9)^{1/2}\langle 2p k_2 p | v0 | \nu_3 p 2p \rangle - (1/1125)^{1/2}\langle 2p k_2 p | v2 | \nu_3 p 2p \rangle - (5/9)^{1/2}(\epsilon_{2p}^{1S} - \frac{1}{2}k_2^2)\langle k_2 p | 2p \rangle \langle 2p | k_1 p \rangle$
	$^3P k_1 p \to {}^1S \nu_3 p$	$-\langle 2p \nu_3 p | v0 | k_1 p 2p \rangle + \frac{1}{5}\langle 2p \nu_3 p | v2 | k_1 p 2p \rangle - (\epsilon_{2p}^{1S} - \frac{1}{2}k_1^2)\langle \nu_3 p | 2p \rangle \langle 2p | k_1 p \rangle$

a $\langle k l n l | v \kappa | k' l' n l \rangle = \int_0^\infty \int_0^\infty f_{kl}(r_1) f_{k'l}(r_1)(r_<^\kappa / r_>^{\kappa+1}) P_{nl}(r_2) P_{n'l}(r_2) dr_1 dr_2$.

b $\langle k l | n l \rangle = \int_0^\infty f_{kl}(r_1) P_{nl}(r_1) dr_1$.

c Λ_1 and Λ_2 are symbolic of a series of terms that are quite small.

excited state in electron-ion scattering. Recent configuration-interaction close-coupling work[6] yields an energy of $\epsilon_\nu = 3.83$ eV for the OII ^3D $3s$ $^2D^o$ state, while isoelectronic extrapolations of experimental energies place the energy at $\epsilon_\nu = 3.63$ eV.[13] Since our aim is to calculate the cross section, we used the "experimental" energy to position the $3s$ $^2D^o$ resonance as accurately as possible.

Using Eqs. (13) and (14) and Table II, we computed the S^Γ matrix elements for the three-channel $^2D^o$ partial wave. Results for components of the reactance matrix $\Re^\Gamma \cong (S^\Gamma - 1)/2i$ are given in Table III at various incident electron energies. We computed $\sigma(^2D^o, p \to p)$ in the low-energy region using Eq. (28), and results are shown in Fig. 1 as a solid curve. The nonresonant partial cross section is shown as the dash-dotted curve in Fig. 1. Also shown in Fig. 1 is a configuration-interaction close-coupling result of Eissner and Seaton.[6] The difference in the positions of the peak heights is due to the use of different energies for the $3s$ $^2D^o$ state. If we had used the close-coupling energy of $\epsilon_\nu = 3.83$ eV, instead of the "experimental" value of $\epsilon_\nu = 3.63$ eV, the two curves would have lined up much more favorably. If we had used the distorted-wave energy of $\epsilon_\nu = 4.20$ eV, our curve would have peaked even further to the right of the Eissner and Seaton result. As shown by Fig. 1, the distorted-wave method, when applied to resonance structures for electron-ion scattering as outlined in Sec. II, is in good agreement with the more elaborate close-coupling method.

In the low-energy region from the ^1D threshold to 5.0 eV, the $\sigma(^2P^o, p \to p)$ partial cross section contains a series of resonances due to the accessibility of OII $1s^2 2s^2 2p^2$ ^1S np $^2P^o$ autoionization states. The $5p$, $6p$, and $7p$ orbitals were calculated using Eq. (3) and Table I and were found to have energies of $\epsilon_\nu = 2.68$, 3.56, and 4.07 eV, respectively, relative to the ^3P ground state. The threshold for the opening of the $1s^2 2s^2 2p^2$ ^1S channel is at 5.35 eV.[13] Using a quantum-defect extrapolation from the experimental energy of the OII ^1S $3p$ $^2P^o$ state ($\epsilon_\nu = -4.13$ eV[13]) gives the np ($n = 5 \to 7$) orbital energies $\epsilon_\nu = 2.58$, 3.51, and 4.04 eV. The $5p$ $^2P^o$ state lies only 0.07 eV above the ^1D excitation threshold. We again use these "experimental" energies to position the resonances as accurately as possible.

The S^Γ matrix elements for the three-channel $^2P^o$ partial wave were calculated using Eqs. (13) and (14) and Table II. Results for the reactance matrix are given in Table III at various incident electron energies. Using Eq. (28), we found the resonance structures in the $\sigma(^2P^o, p \to p)$ excitation cross section to have smaller peak heights and

TABLE III. Reactance matrix and phase shifts.

Partial wave	Energy (eV)	$\mathcal{R}_{21}{}^{a}$ $^{3}Pk_1p \to {}^{1}Dk_2p$	$\mathcal{R}_{23}$ $^{3}D\nu_3s \to {}^{1}Dk_2p$	$\mathcal{R}_{31}$ $^{3}Pk_1p \to {}^{3}D\nu_3s$	Phase shift ^{b} $^{3}Pk_1p$
$^{2}D^{o}$	3.0	0.2447	0.2137	−0.0543	1.2951
	4.0	0.2436	0.2260	−0.0642	1.2847
	5.0	0.2424	0.2405	−0.0740	1.2778
		$\mathcal{R}_{21}{}^{a}$ $^{3}Pk_1p \to {}^{1}Dk_2p$	$\mathcal{R}_{23}$ $^{1}S\nu_2p \to {}^{1}Dk_2p$	$\mathcal{R}_{31}$ $^{3}Pk_1p \to {}^{1}S\nu_3p$	
$^{2}P^{o}$	2.6	−0.2308	−0.0083	0.1322	1.1636
	3.4	−0.2305	−0.0073	0.1262	1.1586
	3.9	−0.2302	−0.0072	0.1225	1.1555

$^{a}\mathcal{R}^{\Gamma} \cong (\mathcal{S}^{\Gamma} - 1)/2i$ where $\mathcal{S}^{\Gamma}$ is defined by Eqs. (13)–(19).
^{b}Non-Coulomb phase shift δ is defined by Eq. (4).

narrower widths when compared to the close-coupling results.[6] This is probably due to inaccuracy in the $\mathcal{S}_{23}^{\Gamma}$ matrix element between the ground configuration ^{1}D and ^{1}S channels since its calculation involves an almost complete cancellation between the quadrupole direct term and the other exchange terms (see Table II).

The total excitation cross section for the $^{3}P \to {}^{1}D$ transition in doubly ionized oxygen is shown in Fig. 2 from the ^{1}D threshold to 5.0 eV. The partial cross sections $\sigma(^{2}D^{o}, p \to p)$ and $\sigma(^{2}P^{o}, p \to p)$ containing resonance structures have been added to $\sigma(^{2}F^{e}, d \to d)$ and $\sigma(^{2}P^{e}, d \to d)$ to give the solid curve shown. Resonances due to the $3s$ $^{2}D^{o}$ and $5p$ $^{2}P^{o}$ through $12p$ $^{2}P^{o}$ autoionization states are clearly seen. There are no resonances in the $d \to d$ cross sections in this energy region.[6] From

previous work[5] we estimate that the remaining contribution from all other partial waves is quite small, though there may be narrow spikes due to resonances. Also shown in Fig. 2 is the total nonresonant cross section (dash-dotted curve) and the total resonance-averaged cross section obtained using Eq. (30) (dotted curve).

Electron-impact excitation-rate coefficients, involving the integration of the cross section over a Maxwell-Boltzmann distribution of electron velocities, are required for astrophysical and laboratory plasma work. For a temperature of 10 000°K the mean energy of the electron distribution is only 1.10 eV. The cross section for oxygen III $^{3}P \to {}^{1}D$, with a threshold at 2.51 eV, then falls completely in the exponential tail of the electron-energy distribution. For cool plasma tempera-
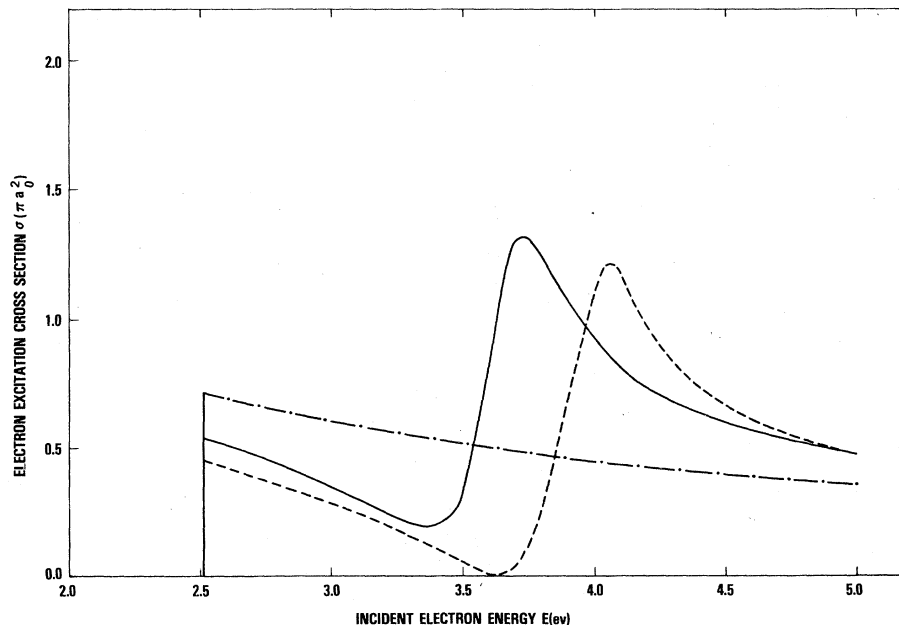

FIG. 1. $\sigma(^{2}D^{o}, p \to p)$ partial-wave cross section for the $^{3}P \to {}^{1}D$ electron excitation of oxgen ɪɪɪ. (——) distorted-wave method including resonances; (—·—) distorted-wave method, nonresonant background; (---) configuration-interaction close-coupling method of Eissner and Seaton (Ref. 6).
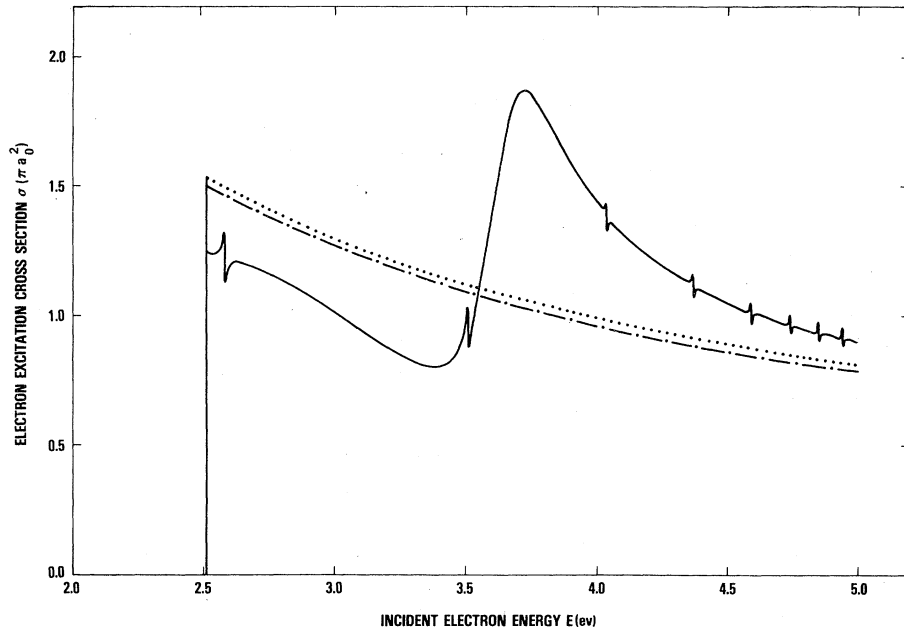
FIG. 2. Total cross sec-
tion for the $^3P \rightarrow ^1D$ electron
excitation of oxygen III.
(——) distorted-wave method
including resonances;
(—·—) distorted-wave
method, nonresonant back-
ground; (·····) distorted-
wave method, resonance-
averaged cross section.

tures below $10\,000\,°K$, found in gaseous nebulae
and the Earth's ionosphere, the difference between
the resonance and resonance-averaged cross
sections (see Fig. 2) from threshold to 3.5 eV has
a quite significant effect on the rate coefficient.
Isolated resonance effects, as opposed to the
resonance-averaged cross section, may thus
prove essential in determining rate coefficients for
certain temperature ranges in electron-ion scat-
tering.

In Fig. 3 we extend the total nonresonant dis-

torted-wave cross section to 30.0 eV (dash-dotted
curve) and compare with a distorted-wave calcula-
tion of Davis and Blaha.[14] For comparison, the
total cross section including resonances is shown
as the solid curve from threshold to 5.0 eV. If
the total cross section including resonances was
extended to 30.0 eV, we would find resonance
structure to be present over the complete energy
range since the ionization potential of oxygen III
is 54.93 eV.[13] For even more highly charged ions,
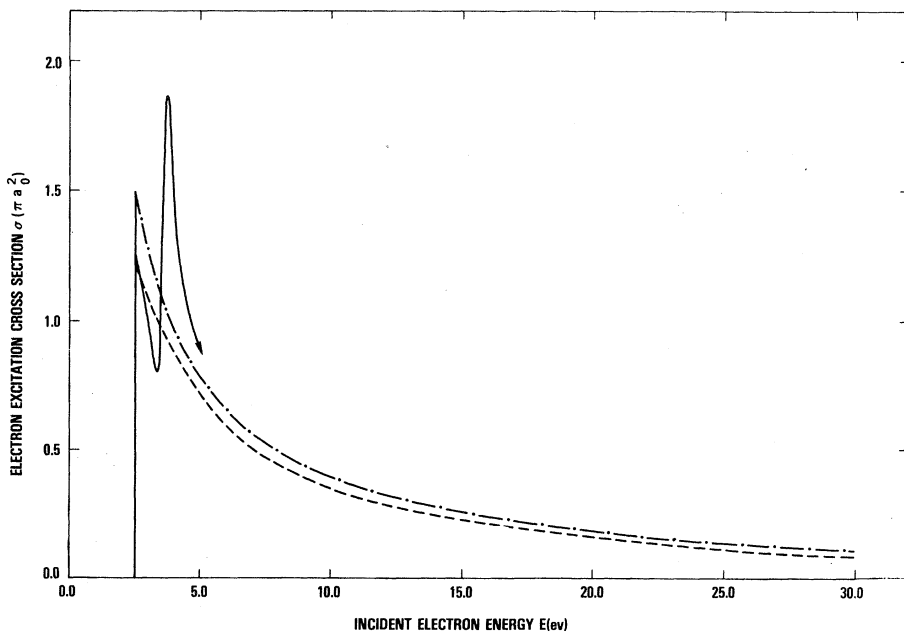the multitude of closed channels that may contri-

FIG. 3. Total cross sec-
tion for the $^3P \rightarrow ^1D$ electron
excitation of oxygen III.
(——) distorted-wave method
including resonances;
(—·—) distorted-wave
method, nonresonance back-
ground; (---) distorted-wave
approach of Davis and Blaha
(Ref. 14).

bute resonance effects makes clear the need for a distorted-wave method approach.

IV. SUMMARY

It can be concluded that the distorted-wave method based on a fully consistent incorporation of electron-exchange effects can be used quite effectively in calculating electron-excitation cross sections of positive ions. Resonance structures may be calculated in the distorted-wave approximation in a very natural way through the use of quantum-defect theory. For the $^3P \rightarrow {}^1D$ electron excitation of oxygen III the agreement between the distorted-wave method and a configuration-interaction close-coupling calculation was found to be quite good even at energies very near threshold. In the future we hope to apply the distorted-wave method to electron-ion scattering problems of general interest.

[1] M. J. Seaton, *Advances in Atomic and Molecular Physics* (Academic, New York, 1975), Vol. II, p. 83.

[2] M. K. Gailitis, Usp. Fiz. Nauk. 116, 665 (1975) [Sov. Phys.-Usp. 18, 600 (1976)].

[3] M. D. Hershkowitz and M. J. Seaton, J. Phys. B 6, 1176 (1973).

[4] L. P. Presnyakov and A. M. Urnov, Zh. Eskp. Teor. Fiz. 68, 61 (1975) [Sov. Phys.-JETP 41, 31 (1975)].

[5] M. S. Pindzola, A. K. Bhatia, and A. Temkin, Phys. Rev. A 15, 35 (1977).

[6] W. Eissner and M. J. Seaton, J. Phys. B 7, 2533 (1974); [cf. also W. Eissner, H. Nussbaumer, H. E. Saraph, and M. J. Seaton, J. Phys. B 2, 341 (1969)].

[7] N. F. Mott and H. S. W. Massey, *The Theory of Atomic Collisions* (Oxford, New York, 1965).

[8] M. J. Seaton, J. Phys. B 2, 5 (1969).

[9] Y. B. Zeldovich, Zh. Eksp. Teor. Fiz. 39, 776 (1960) [Sov. Phys.-JETP 12, 542 (1961)].

[10] K. Smith, *The Calculation of Atomic Collision Processes* (Wiley, New York, 1971).

[11] M. K. Gailitis, Zh. Eksp. Teor. Fiz. 44, 1974 (1963) [Sov. Phys.-JETP 17, 1328 (1963)].

[12] C. F. Fisher, Comp. Phys. Comm. 1, 151 (1969).

[13] C. E. Moore, *Atomic Energy Levels*, NSRDS-NBS 35 (U.S. GPO, Washington, D.C., 1971).

[14] J. Davis and M. Blaha, Naval Research Lab. Mem. Report 3325, 1976 (unpublished).